DOE/ER/14003--T1

Interspecies acetate transfer influences the extent of anaerobic benzoate degradation by syntrophic consortia.

FY05-89ER14003

Veena Warikoo[1 #], Michael J. McInerney[1 *], Joseph A Robinson[2], and Joseph M. Suflita[1]

[1] Department of Botany and Microbiology, University of Oklahoma, Norman, OK 73019-0245, and

[2] Microbiology and Nutrition Research, The UpJohn Company, Kalamazoo, MI 49001.

Running Title: Acetate inhibition of benzoate degradation.

[*] Corresponding author: Michael J. McInerney
Department of Botany and Microbiology
University of Oklahoma
770 Van Vleet Oval
Norman, OK 73019-0245
Telephone # : 405-325-6050 Fax # : 405-325-7619

[#] Present address: Department of Civil Engineering
Stanford University
Stanford, CA 94305-4020

ABSTRACT

Benzoate degradation by an anaerobic, syntrophic bacterium, strain SB, in coculture with *Desulfovibrio* strain G-11 reached a threshold value which depended on the amount of acetate added, and ranged from about 2.5 to 29.9 μM. Increasing acetate concentrations also uncompetitively inhibited benzoate degradation. The apparent V_{max} and K_m for benzoate degradation decreased with increasing acetate concentration, but the benzoate degradation capacity (V_{max}/K_m) of cell suspensions remained comparable. The addition of an acetate-using bacterium to cocultures after the threshold was reached resulted in the degradation of benzoate to below the detection limit. Mathematical simulations showed that the benzoate threshold was not predicted by the inhibitory effect of acetate on benzoate degradation kinetics. With nitrate instead of sulfate as the terminal electron acceptor, no benzoate threshold was observed in the presence of 20 mM acetate even though the degradation capacity was lower with nitrate than with sulfate. When strain SB was grown with a hydrogen-using partner that had a 5-fold lower hydrogen utilization capacity, a 5 to 9-fold lower the benzoate degradation capacity was observed compared to SB/G-11 cocultures. The Gibb's free energy for benzoate degradation was less negative in cell suspensions with threshold compared to those without threshold. These studies showed that the threshold was not a function of the inhibition of benzoate degradation capacity by acetate, or the toxicity of the undissociated form of acetate. Rather a critical or minimal Gibb's free energy may exist where thermodynamic constraints preclude further benzoate degradation.

INTRODUCTION

The anaerobic degradation of aromatic compounds involves the concerted action of many microbial species (18, 26, 54. The initial transformations of aromatic compounds often involve the alteration of substituent groups, or ring activation reactions to hydroxylated, carboxylated, or amino derivatives (19). The latter three functional groups and halogens are often removed prior to ring reduction and cleavage. Many times, the result of these transformations is the conversion of diverse aromatic substrates to benzoic acid. Thus, the factors that influence the rate and extent of benzoate degradation may also influence the anaerobic biodegradation of other aromatic compounds.

In methanogenic environments, benzoate is degraded to acetate, H_2, and formate, by syntrophic bacteria (18, 34, 45, 49). The degradation of benzoate is thermodynamically unfavorable unless the reaction is coupled to the use of hydrogen and/or formate by organisms such as methanogens (18, 30, 34). We have isolated a new bacterium, strain SB, that degrades benzoate only in coculture with a H_2/formate-using bacterium such as *Desulfovibrio* strain G-11 according to equation 1 (24).

$$\text{benzoate}^- + 6\ H_2O \text{ --------> } 3\ \text{acetate}^- + HCOO^- + 2\ H_2 + 3\ H^+ \qquad (1)$$

$$\Delta G^{0'} = 69.2 \text{ kJ/mol (26)}$$

Recently, we showed that SB/G-11 cocultures degrade benzoate to a threshold concentration below which no further benzoate degradation occurs, even after extended incubations (24).

Thresholds for the biodegradation of synthetic and natural organic compounds (8, 12, 20, 38, 53), for the utilization of inorganic nutrients (12), and for anaerobic hydrogen utilization (14, 29) have been reported. The existence of thresholds may explain the persistence of trace levels of many organic compounds in natural waters (25). Little is known about the causes of thresholds. The threshold value for benzoate degradation by the SB/G-11 coculture seemed to be thermodynamically controlled since increased acetate concentrations increased the benzoate threshold value (24). However, there are other possible explanations for the existence of the benzoate threshold. Toxic levels of the undissociated form of acetate have been postulated as the cause of acetate thresholds in pure cultures of acetoclastic methanogens and in acclimatized sludge (20, 21). Small increases in the levels of hydrogen and/or formate can inhibit the degradation of ethanol and volatile fatty acids by defined syntrophic consortia and environmental samples (1, 10, 17, 23, 31, 36, 47, 52). High concentrations of acetate are also known to inhibit the substrate degradation by syntrophic consortia (1, 6, 10, 16). Further study of the causes of substrate thresholds will be important in understanding the factors that affect the fate of natural and synthetic chemicals in the environment.

We sought to determine if the benzoate threshold was due to: i) the inhibition of benzoate degradation kinetics by acetate, ii) the toxicity the undissociated form of acetate, or iii) the result of thermodynamic limitations. We also examined the effect that different H_2 utilization kinetics had on the rate of benzoate degradation by defined syntrophic cocultures.

MATERIALS AND METHODS

Organisms and growth conditions. A syntrophic, benzoate degrader, strain SB, was isolated from sewage sludge (24). *Desulfovibrio* strain DG2 was kindly provided by J. M. Tiedje, East Lansing, MI. A basal medium (24, 32) with 10 mM sodium benozate, 30 mM sodium sulfate, 2% (vol/vol) clarified rumen fluid, and an 80% N_2 : 20% CO_2 gas phase was used for the growth of strain SB in coculture with either *Desulfovibrio* strain G-11 or *Desulfovibrio* strain DG2. Pure cultures of *Desulfovibrio* strain G-11 and *Desulfovibrio* strain DG2 were grown in the basal medium with 10 mM sodium sulfate and 80% H_2 : 20% CO_2 gas phase. Pure cultures of *Desulfoarculus baarsii* (DSM 2075) was grown in the basal medium with 10 mM each of sodium sulfate and sodium acetate and an 80% N_2 : 20% CO_2 gas phase.

Methods for the preparation and use of anaerobic media and solutions were essentially those of Bryant (11) and modified by Balch and Wolfe (5). All cultures were incubated at 37°C. Cultures with hydrogen in the gas phase were incubated on their sides on a rotary shaker, and the headspace of the bottles was repressurized every 2 to 3 days. The purity of cultures was checked routinely by microscopic examination, Gram reaction and inoculation of thioglycolate broth (Difco Laboratories, Inc., Detroit, MI). Growth was monitored by change in absorbance at 600 nm (35).

Cell suspensions. Cells of the benzoate-degrading cocultures of SB/G-11 and SB/DG2 were concentrated prior to kinetic experiments. All manipulations of cells were done inside an anaerobic chamber, which contained 1 to 5% of H_2 with the balance being N_2. About 3 liters of the coculture were grown to mid-exponential phase of growth, harvested by centrifugation (1200 x g, 20 min, 4°C), and washed three times with 50 mM sodium phosphate buffer (pH 7.5) prior to being resuspended in 100 ml of the basal medium containing 0.2 to 0.3 mM sodium benzoate and 1 mM sodium sulfate, but

without vitamins and rumen fluid. The cell suspension was transferred to 160-ml serum bottles which were closed with black rubber stoppers.

Similarly, pure cultures of sulfate reducers were grown to mid-exponential phase harvested by centrifugation. *D. baarsii* cells were washed three times as above. The final cell pellet was placed on ice in the anaerobic glove box. Cell pellets of *Desulfovibrio* strains G11 and DG2 were washed twice with anoxic piperazine-N,N'-bis-2-ethanesulfonic acid (PIPES) buffer (50 mM, pH 7.0), resuspended in 45 ml of the same buffer, and dispensed into 160-ml serum bottles, which were sealed with black rubber stoppers. The head space in each bottle was adjusted to 100% N_2 (30 kPa).

Benzoate kinetics. Kinetic experiments were designed to follow substrate depletion through the zero-, mixed-, and first-order regions using at least duplicate cell suspensions. Each cell suspension was amended with anoxic solutions of sodium benzoate, sodium sulfate or sodium nitrate and 1-ml samples were periodically withdrawn for analysis. To determine the effect of acetate on benzoate degradation, duplicate cell suspensions were amended with sodium benzoate (200 to 300 μM), sodium sulfate (1 mM), and sodium acetate (0 to 65 mM). Control cell suspensions received 65 mM sodium chloride instead of sodium acetate. Acetate, formate, and hydrogen were quantified when the concentration of benzoate either reached a threshold value, or was degraded to below the HPLC detection limit (0.2 μM).

H_2 kinetics. Duplicate cell suspensions of *Desulfovibrio* strains G-11 or DG2 were amended with an anoxic solution of sodium sulfate to give an initial concentration of 2 mM. Hydrogen was added to each serum bottle with a syringe to give an overpressure of 60 to 70 kPa. The serum bottles were then incubated at 35°C with agitation in an orbital shaker at 200 rpm. Autoclaved cell suspensions and buffer without cells served as controls. The gas pressure was measured using a pressure transducer, and changes in transducer output were processed through a switching circuit and digital-analog input-output module to a computer (15). A standard curve relating the

amount of H_2 added to the serum bottle versus pressure showed that the transducer response was linear up to 110 kPa. Also, the electrical output of the pressure transducer was proportional to the gas pressure in the serum bottle (1 mv/kPa). H_2 consumption rates were determined by converting the gas pressure measurements into μmoles of H_2 (35) as a function of time. The rate of the H_2 use (in μmoles) was normalized to the amount of total protein present in bottles. In some serum bottles the concentration of hydrogen was measured directly with a gas chromatograph equipped with mercury vapor detector (41) to confirm the accuracy of the pressure transducer data.

Acetate removal experiment. Cell suspensions of strain SB and *Desulfovibrio* strain G-11 amended with 200 to 300 μM benzoate, 1 mM sulfate, and 20 mM acetate were incubated until a benzoate threshold value was reached. The washed cell pellet of *D. baarsii* was then added to duplicate cell suspensions of the coculture to form a defined triculture. The SB/G-11 cell suspensions not inoculated with *D. baarsii* served as controls.

Model discrimination. Since the protein concentration did not change during the progress curve experiments (data not shown), mathematical models not linked to growth (3, 4) were used to estimate kinetic parameters. A modified second-order model (48) was also tested for the case where a small increase in biomass occurred during the experiment, but was undetected by the protein determination method. The modified second-order model could not be used because no convergence was achieved when this model was fit to various sets of progress curve data. The integrated forms of Michaelis-Menten model (equation 2), the first-order model (equation 3) were tested to determine the model that best described the progress curve data:

$$V_{max}\, t = S_o - S + K_m \ln (S_o/S) \qquad (2)$$

$$S = S_o \exp (-V_{max}/K_m\, t) \qquad (3)$$

V_{max} is the maximum rate of substrate consumption (in nmol minute^{-1} mg^{-1} protein), K_m is the half-saturation constant (in μM), S is the substrate concentration (in μM), t is the time (in minutes), and S_o is the initial substrate concentration (in μM).

In experiments where a benzoate threshold concentration was observed, the modified versions of the integrated forms of Michaelis-Menten model (equation 4) and the first-order model (equation 5) that included threshold terms were used:

$$V_{max}\, t = S_o - S + (K_m + S_c) \ln (S_c - S_o/S_c - S) \quad (4)$$

$$(S_c - S) = (S_c - S_o) \exp [-V_{max}/(K_m + S_c)\, t] \quad (5)$$

In equations 4 and 5, S_c is the threshold concentration (in μM).

The criteria used to assess the goodness-of-fit of the above models (equations 2-5) were: a) the model with lowest standard error associated with each parameter estimate, and b) the model that had residual plots with a random distribution of an equal number of positive and negative values about the zero level. Based on these criteria, the integrated form of Michaelis-Menten model (equation 2) or its modified version (equation 4) was superior to the other models and was used to estimate the kinetic parameters of benzoate degradation from the progress curve data.

Plots of the sensitivity equations of equations 2 and 4 using data in the first-, mixed- and zero- order regions showed that the curves generated for the three regions were not multiples of each other (data not shown). Thus, these two equations provided unique estimates of the kinetic parameters.

Inhibition model. Estimates of the Michaelis constants associated with benzoate degradation by Lineweaver-Burk double reciprocal plots suggested that

benzoate degradation was inhibited in the presence of acetate (data not shown). Equations 2 and 4 were modified to account for competitive, noncompetitive, uncompetitive, and mixed types of inhibition (39) to obtain estimates of the inhibition constant (K_i). Initial parameter estimates (V_{max} and K_m) were obtained using equation 2 and data from experiments without acetate added to the cell suspensions. Equations 2 and 4 modified for the four types of inhibition were each solved for S versus t with different initial acetate concentrations, using the actual values for S_o and S_c the above estimates of V_{max} , K_m, and K_i. The substrate decay curves generated from each of simulations were compared to the respective experimental data to determine which model accurately predicted the mode of acetate inhibition.

Parameter estimation. The least squares method was used for data analysis using integrated form of Michaelis-Menten model (equation 2) and its modified version (equation 4) using the Levenberg-Marquardt algorithm (7) All regression analyses were done with an Macintosh Quadra 650 microcomputer (Apple computer, Inc., Cupertino, CA) using Mathcad (MathSoft Inc., Cambridge, MA) to perform nonlinear regression analysis.

Analytical methods. Samples were centrifuged at 12,000 x *g* for 4 min prior to analysis by high pressure liquid chromatography. The concentration of benzoate was determined using a high pressure liquid chromatography (HPLC) system equipped with a C_{18} reverse phase column (250 mm x 4.6 mm, 5 microns) and an ultraviolet (uv) detector set at 271 nm. HPLC was operated at a flow rate of 1.2 ml/min using a mobile phase of 80% sodium acetate (50 mM; pH 4.5) and 20% acetonitrile. The detection limit for benzoate was 0.2 μM. The concentration of acetate was also determined with a HPLC equipped with an ion exclusion column (300 x 7.8 mm) and a fixed wavelength uv detector (214 nm). A flow rate of 1 ml/min of 0.03 N H_2SO_4 was used. Identification and quantitation of the eluting compounds were made by comparison with authentic external standards.

The formate concentration was determined spectrophotometrically using a duel-beam instrument operated in the time-course mode. The assay is based on measuring the increase in absorbance at 340 nm due to formate dehydrogenase (FDH)-catalyzed production of NADH from formate and NAD^+. FDH (from yeast), NAD^+, and NADH solutions were prepared in 50 mM HEPES (N-2 hydroxyethylpiperazine N'-2-ethanesulfonic acid) buffer at pH 7.6. Basal medium was used in the reference cuvette as a blank. Medium containing a known amount of formate or without the addition of NAD^+ served as controls. After the addition of 20 µl of 100 mM NAD^+ solution to the sample, the background absorbance was monitored for 2 to 3 min. The assay was started by the addition of 100 µl of 50 units per ml FDH solution. The reaction was followed until no further change in absorbance occurred. A standard curve for NADH in medium (molar extinction coefficient of 5.33×10^3) was generated. The concentration of formate was calculated from the ΔA_{340} and the NADH standard curve. The detection limit of the assay was 0.5 µM.

Whole cell protein was determined using bovine serum albumin as the standard as described previously (29). The samples and the standards were boiled in 0.1 N NaOH for 20 min to digest the cells prior to protein determination.

Energetics. At the end of each kinetic experiment, the pH, temperature, and concentrations of benzoate, acetate, formate, and H_2 were determined. The Gibb's free energy ($\Delta G^{0'}$) for benzoate degradation under non-standard conditions was calculated using the measured concentrations of reactants and products according to equation 6.

$$\Delta G^0 = \Delta G^{0'} + RT \ln \frac{(CH_3COO^-)^3 \, (H_2)^2 \, (HCOO^-)}{(C_6H_5COO^-)} \qquad (6)$$

where (H_2) is the H_2 partial pressure (in atm), and the values in brackets are the molar concentrations of the respective compounds. The standard Gibb's free energy (ΔG^o) for benzoate degradation was calculated from the data in Kaiser and Hanselmann (26).

RESULTS

Effect of acetate on benzoate decay. Figure 1 shows representative progress curves for benzoate degradation by cell suspensions of SB/G-11 with and without a sodium acetate amendment. Without the amendment, benzoate was degraded to the detection limit. With 20 mM sodium acetate, the rate of benzoate degradation by the coculture was inhibited and a threshold benzoate concentration was observed. After the threshold was reached, no further benzoate degradation was observed an even with extended incubation (14 days).

Experimental manipulation of the acetate concentration (20.0 and 65.7 mM) resulted in benzoate threshold concentrations of 2.3 μM and 29.8 μM, respectively (Table 1). In the cell suspensions amended with ≤10 mM sodium acetate or with 65 mM NaCl, benzoate was degraded to the detection limit (Table 1). The change in Gibb's free energy ($\Delta G'$) for benzoate degradation was favorable in all cell suspensions including those with a benzoate threshold. However, $\Delta G'$ for benzoate degradation was less in the cell suspensions without threshold (Table 1).

When an acetate-using sulfate reducer, *Desulfoarculus baarsii,* was added to cell suspensions of SB/G-11 that had degraded benzoate to a threshold concentration (7.1 μM), a decrease in both the acetate and benzoate concentrations was observed (Table 2). In comparable cell suspensions that did not receive *D. baarsii,* benzoate was degraded to a threshold value of 3.7 μM (Table 2).

In cell suspensions amended with different concentrations of sodium acetate, the apparent V_{max} for benzoate degradation decreased with increasing acetate

concentrations (Table 3). However, this decrease in V_{max} was offset by a reduction in the apparent K_m for benzoate degradation such that the specific benzoate degradation capacity (V_{max}/K_m) remained comparable in all cell suspensions (Table 3). In cell suspensions amended with 65 mM sodium chloride, the apparent kinetic constants for benzoate degradation were similar to those from cell suspensions without acetate.

Competitive, noncompetitive, uncompetitive, and mixed inhibition models mathematically modified to account for a threshold predicted K_i values of 43.2, 107, 10.0, and 16.8 mM, respectively. Regardless of whether cell suspensions were amended with 10, 20 or 65 mM acetate, the decrease in the apparent V_{max} and K_m for benzoate degradation was $\geq$ 50 % (data not shown), indicating that the actual K_i for acetate must be $\leq$ 10 mM. Figure 2 compares the actual and simulated benzoate decay curves predicted by the four inhibition models with 65 mM acetate, assuming a K_i value of 10 mM. Only the uncompetitive inhibition model accurately simulated the experimental data. A reduction in both the apparent V_{max} and K_m (Table 3) is also consistent with an uncompetitive type of inhibition. Similar results were obtained when simulated and actual benzoate decay curves were compared with initial acetate concentrations of 10 mM and 20 mM (data not shown). Therefore, it is most likely that acetate functioned as an uncompetitive inhibitor with a K_i value of 10.0 $\pm$ 0.6 mM. None of the inhibition models accurately described the course of benzoate decay if they failed to account for the threshold, as illustrated in Figure 3 for the uncompetitive inhibition model. This was true even if an initial acetate concentration up to 100 mM was used, or when values for V_{max}, K_m ,and K_i were increased or decreased by 50% of the estimated values (data not shown).

Effect of the terminal electron acceptor on the threshold. Cell suspensions of SB/G-11 amended with 20 mM acetate and the terminal electron acceptor, nitrate, degraded benzoate to below the detection limit (Table 4). In contrast, comparable incubations containing sulfate as the electron acceptor exhibited the expected benzoate

threshold (Table 4). Since both suspensions received the same initial amount of sodium acetate, the concentration of the undissociated form of acetate was the same in both the cases. However, a benzoate threshold value was observed only when the thermodynamically less favorable electron acceptor, sulfate, was used. This was true even though the benzoate uptake capacity was 50% lower in suspensions containing nitrate rather than sulfate as the electron acceptor (Table 4).

Effect of hydrogen utilization capacity on benzoate degradation. The kinetic parameters for H_2 use by pure cultures of *Desulfovibrio* strains G-11 and DG2 were determined by nonlinear regression analysis. The apparent V_{max} and K_m for H_2 utilization were 145 ± 1.2 nmol min^{-1} mg^{-1} and 1.2 ± 1.2 μM for strain G-11, and 34.4 ± 2.8 nmol min^{-1} mg^{-1} and 1.4 ± 0.4 for strain DG, respectively. The apparent V_{max} and K_m for both strains were comparable to values previously reported (40). The H_2 removal capacity of *Desulfovibrio* strain G-11 was 120.8 min^{-1} which was five times higher than that of *Desulfovibrio* strain DG2, 24.5 min^{-1}.

To determine the effect of hydrogen removal capacity on the rate of benzoate degradation, strain SB was grown with either *Desulfovibrio* strain DG2 or strain G-11. The rate of benzoate degradation decreased 37-fold when strain DG2 was the syntrophic partner of strain SB (Table 5). These data show that the rate of benzoate degradation is controlled by the rate of H_2 use by the syntrophic partner. The $\Delta G'$ for benzoate degradation in the coculture of SB/DG2 was comparable to the $\Delta G'$ in SB/G-11 coculture (Table 5).

DISCUSSION

The inhibitory effects of acetate on kinetics of benzoate degradation by SB/G-11 cocultures could not be adequately explained by a variety of inhibition models unless a term for a benzoate threshold value was included (Fig. 2 and 3). The fact that very high

acetate levels (about 80 mM) inhibit propionate (27) and butyrate (1, 6) suggests that thresholds for the degradation of these substrates may also exist. Although Dolfing and Tiedje (16) showed that acetate inhibited the rate of benzoate degradation by a defined syntrophic consortia, a threshold for benzoate degradation was not observed probably because the rate of benzoate degradation was calculated from the rate of methane production. Thus, it is not known if benzoate was completely degraded. Acetate most likely acted as an uncompetitive inhibitor of benzoate degradation in our cocultures with an apparent K_i of 10 mM. Dolfing and Tiedje (16) found an apparent K_i of 40 mM for acetate inhibition of benzoate degradation by a different syntrophic bacterium in coculture with a methanogen. The K_i for acetate inhibition of propionate degradation (8.3 mM at pH of 7.0) (21) was very similar to the K_i for benzoate degradation reported here.

Several lines of evidence suggest that the threshold for syntrophic benzoate degradation was thermodynamically controlled rather than the result of acetate inhibition or toxicity. Both the apparent V_{max} and K_m for benzoate degradation decreased with increasing acetate concentrations (Table 3). Thus, little or no change in benzoate degradation capacity occurred since the decrease in V_{max} was offset by an increase in the affinity for benzoate. Another possible explanation for the benzoate threshold is that high acetate concentrations may severely inhibit the rate of benzoate degradation when benzoate concentrations are low so that little or no change in benzoate concentration occurs. Simulation studies based on a variety of inhibition models did not predict a benzoate threshold, even when initial acetate concentration and the values for V_{max}, K_m ,and K_i were varied within reasonable limits. Thus, a kinetic explanation for the benozate threshold is extremely unlikely.

Toxicity of the undissociated form of acetate cannot be the reason for a benzoate threshold since a threshold was not observed when nitrate substituted for sulfate as an electron acceptor, even though both suspensions had the same initial amendment of

acetate (Table 4). The build up of inhibitory levels of hydrogen is not responsible for a benzoate threshold since hydrogen levels were about 0.4 Pa (Table 1). Such H_2 levels are below that found in other syntrophic associations (1, 17, 52). Also, an increase in the H_2 partial pressure from 0.25 Pa to 0.85 Pa did not inhibit the rate of benzoate in a cell suspension of SB/G-11 (data not shown). Similarly, the buildup of formate to inhibitory levels (10, 52) can be excluded as a cause for the benzoate threshold since formate concentrations did not differ in cocultures with or without a threshold (Table 1).

Consistent with a thermodynamic explanation, the benzoate threshold value was influenced by the initial acetate concentration (24) (Table 1), the amount of benzoate added (24), and consequently the amount of acetate produced. The addition of an acetate-utilizing bacterium to cell suspensions with a benzoate threshold resulted in acetate degradation and further degradation of benzoate (Table 2). This result would be expected if the threshold was thermodynamically controlled since a decrease in the concentration of an end product would tend to pull the reaction in the forward direction. Moreover, no threshold was observed when a thermodynamically more favorable electron acceptor was used, even though the overall kinetics of benzoate degradation were much slower with nitrate rather than sulfate as the electron acceptor (Table 4).

Calculations showed that the degradation of benzoate was thermodynamically favorable in cell suspensions exhibiting a threshold although the $\Delta G'$ was more negative in comparable cell suspensions without a threshold (Table 1). It may be that there is a "critical" Gibb's free energy (ΔG_c) value, above which no further benzoate degradation can occur. A value of about 17 to 23 kJ has been proposed as the minimum energy quantum needed to conserve energy in a living cell (42, 50). This corresponds to the amount of energy needed to translocate one mole of protons through a fully energized membrane, equivalent to about 1/3 to 1/4 mole of ATP (42). The Δ G' for benzoate degradation when the threshold was reached is close to the value for the minimum energy quantum (Table 1). The threshold may represent the point at which the free

energy change associated with benzoate degradation is not sufficient to allow energy conservation by the cell. A critical Gibb's free energy value has been reported for ethanol degradation by a syntrophic coculture of *Pelobacter acetylinicus* (43, 44), and for hydrogen use (13).

An important implication of the present work is that the extent of benzoate degradation can be estimated from thermodynamic considerations. In syntrophic associations, increases in hydrogen and/or formate are often the reason for inhibition of growth and substrate degradation (1, 10, 17, 23, 36, 47, 52). Here, we show that an increase in acetate concentration, even when hydrogen and formate levels are low, affects the extent of benzoate degradation in defined syntrophic cultures. If a critical ΔG_c for benzoate degradation exists, then the ratio of acetate to benzoate at which the $\Delta G' = \Delta G_c$ can be used to predict the threshold value, assuming that hydrogen and formate levels are low. When equation 6 is solved for the threshold benzoate concentration at a given acetate concentration by assuming $\Delta G' = \Delta G_c$ (-30 kJ/mol) and using the hydrogen and formate concentrations of incubations with thresholds (Table 1), the following relationship is obtained:

$$(\text{benzoate}^-) = 0.13\,(\text{acetate}^-)^3 \qquad (7)$$

Figure 4 shows that a fairly good agreement exists between the experimental threshold values and the values predicted by the above relationship.

From a practical standpoint, the above relationship could be modified to predict the lowest concentration to which an aromatic compound or a volatile fatty acid can be degraded under methanogenic conditions. The influence of acetate on the energetics of benzoate degradation indicates that optimal degradation of benzoate will occur when an active acetate-consuming population exists. The addition of various monocarboxylic acids such as propionate or butyrate dramatically decreased the lag and increased the

rate of benzoate metabolism in lake sediments (46), and stimulated the degradation of mono- and di-chlorophenoxyacetates in anaerobic aquifer samples (22), suggesting that stimulating the activity of terminal trophic groups enhances the activity of aromatic degraders. Theile et al. (51) noted that the selection of different syntrophic bacteria and acetate-using methanogens may be the reason for the improved rates of volatile fatty acid degradation in their granules. These studies and the work reported here suggest that both the rate and extent of substrate degradation by syntrophic consortia are controlled by the efficient removal of endproducts. In particular, we highlight the importance of interspecies acetate transfer.

Cocultures of syntrophic bacteria appear to act as a single organism with the combined metabolic activities of both bacteria. Powell (37, 38) developed a theory that explains the tight coupling between the syntrophic partners based on H_2 production and consumption kinetics. According to this theory, the specific growth rate of the syntrophic coculture depends largely on the growth rate of the H_2-utilizing partner, and this prediction has been experimentally confirmed in several studies (2, 43, 44). However, it is not clear whether the rate of substrate utilization by the syntrophic bacterium also depends on the H_2 utilization kinetics of the H_2-using partner. Dwyer et al. (17) found that the rate of butyrate degradation was faster when the syntrophic partner was a sulfate reducer which had a higher hydrogen utilization capacity (μ_{max}/K_s) compared to cocultures with a methanogen which had a lower hydrogen utilization capacity. However, since the electron acceptor differed between these two cocultures, the rate of butyrate degradation could have been influenced by the thermodynamic as well as kinetic considerations. Seitz et al. (43) found similar rates of ethanol metabolism by *P. acetylinicus* regardless of which the hydrogen-using bacterium, a methanogen, a sulfate reducer, or an acetogen, was used. We found faster rates of benzoate degradation were observed when SB was grown in coculture with strain G-11 than with

strain DG-2 (Table 5), which shows that the rate of benzoate degradation by strain SB depended on the hydrogen utilization capacity of its partner.

Dolfing and Tiedje (16) proposed that it may be possible to grow a syntrophic bacterium in the absence of a hydrogen-using bacterium by interspecies acetate transfer. They based their proposal on the thermodynamic equivalence of acetate and hydrogen plus formate, combined with the inhibitory effects of acetate on benzoate degradation at ecologically realistic concentrations. Our findings on the importance of interspecies acetate transfer on the rate and extent of substrate degradation by defined syntrophic consortia suggests that such an approach may be feasible.

ACKNOLWLEDGMENTS

We thank N. Q. Wofford for formate determinations.

This work was supported by contract DE-FG05-89ER14003 with the U. S. Department of Energy to M. J. M. and Office of Naval Research Grant N00014-93-1-0847 to J. M. S.

LITERATURE CITED

1. Ahring, B. K., and P. Westermann. 1988. Product inhibition of butyrate metabolism by acetate and hydrogen in a thermophillic coculture. Appl. Environ. Microbiol. 54: 2393-2397.

2. Archer, D. B., and G. E. Powell. 1975. Dependence of the specific growth rate of methanogenic mutualistic cocultures on the methanogen. Arch. Microbiol. 141: 133-137.

3. Atkins, G. L., and I. A. Nimmo. 1973. The reliability of Michaelis constants and maximum velocities estimated by using the integrated Michaelis-Menten equation. Biochem. J. 135: 779-784.

4. Atkins, G. L., and I. A. Nimmo. 1980. Current trends in the estimation of Michaelis-Menten parameters. Anal. Biochem. 104: 1-9.

5. Balch, W. E., and R. S. Wolfe. 1976. New approaches to the cultivation of methanogenic bacteria: 2-mercaptoethanesulfonic acid (HS-CoM)-depenedent growth of *Methanobacterium ruminantium* in pressurized atmosphare. Appl. Environ. Microbiol. 32: 781-791.

6. Beaty, P. S., and M. J. McInerney. 1989. Effects of organic acid anions on the growth and metabolism of *Syntrophomonas wolfei* in pure culture and in defined consortia. Appl. Environ. Microbiol. 55: 977-983.

7. Beck, J, V., and K. J. Arnold. Parameter estimation in engineering and science. Wiley, New York.

8. Boething, R. S., and M. Alexander. 1979. Effect of concentration of organic chemicals on their biodegradation by natural microbial communities. Appl. Environ. Microbiol. 37: 1211-1216.

9. Boone, D. R., and M. P. Bryant. 1980. Propionate-degrading bacterium, *Syntrophobacter wolinii* sp. nov. gen. nov., from methanogenic ecosystems. Appl. Environ. Microbiol. 40: 626-632.

10. Boone, D. R., R. L. Johnson, and Y. Liu. 1989. Diffusion of the interspecies electron carriers H_2 and formate in methanogenic ecosystems and its implications in the measurement of K_m for H_2 and formate uptake. Appl. Environ. Microbiol. 55: 1735-1741.

11. Bryant, M. P. 1972. Commentary on the Hungate technique for culture of anaerobic bacteria. Am. J. Clin. Nutr. 25: 1324-1328.

12. Button, D. K. 1985. Kinetics of nutrient-limited transport and microbial growth. Microbiol. Rev. 49:270-297.

13. Conrad, R., and B. Wetter. 1990. Influence of temperature on energetics of hydrogen metabolism in homoacetogenic, methanogenic, and other anaerobic bacteria. Arch Microbiol. 155: 94-98.

14. Cord-Ruwisch, R., H. J. Seitz, and R. Conrad. 1988. The capacity of hydrogenotrophic anaerobic bacteria to compete for traces of hydrogen depends on the redox potential of the terminal electron acceptor. Arch. Microbiol. 149: 350-357.

15. DeWeerd, K. A., F. Concannon, and J. M. Suflita. 1991. Relationship between hydrogen consumption, dehalogenation, and the reduction of sulfur oxyanions by *Desulfomonile tiedjei*. Appl. Environ. Microbiol. 57: 1929-1934.

16. Dolfing, J., and J. M. Teidje. 1988. Acetate inhibition of methanogenic syntrophic benzoate degradation. Appl. Environ. Microbiol. 54: 1871-1873.

17. Dwyer, D. F., E. Weeg-Aerssens, D. R. Shelton, and J. M. Teidje. 1988. Bioenergetic conditions of butyrate metabolism by a syntrophic, anaerobic bacterium in

coculture with hydrogen-oxidizing methanogenic and sulfidogenic bacteria. Appl. Environ. Microbiol. 54: 1354-1359.

18. Ferry, J. G., and R. S. Wolfe. 1976. Anaerobic degradation of benzoate to methane by a microbial consortium. Arch. Microbiol. 107: 33-40.

19. Fuchs, G. M. E. S. Mohamed, U. Altenschmidt, J. Roch, A. Lach, R. Brackmann, C. Lockmeyer, and B. Oswald. 1994. Biochemistry of anaerobic biodegradation of aromatic compounds. In: C. Ratledge (ed.), Biochemistry of Microbial Degradation, pp. 513-553. Kluiver Academic Publishers, Netherlands.

20. Fukazaki, S., N. Nishio, and S. Nagai. 1990. Kinetics of the methanogenic fermentation of acetate. Appl. Environ. Microbiol. 56: 3158-3163.

21. Fukazaki, S., N. Nishio, M. Shobayashi, and S. Nagai. 1990. Inhibition of the fermentation of propionate to methane by hydrogen, acetate, and propionate. Appl. Environ. Microbiol. 56: 719-723.

22. Gibson, S. A., J. M. Suflita. 1990. Anaerobic biodegradation of 2, 4, 5,-trichlorophenoxyacetic acid in samples from a methanogenic aquifer: stimulation of short-chain organic acids and alcohols. Appl. Environ. Microbiol. 56: 1825-1832.

23. Harper, S. R., and F. G. Pohland. 1986. Recent developement in hydrogen management during anaerobic biological wastewater treatment. Biotech. Bioengin 28:585-602.

24. Hopkins, B. T., M. J. McInerney, and V. Warikoo. 1994. Evidence for an anaerobic syntrophic benzoate degradation threshold and isolation of the syntrophic benzoate degrader. Appl. Environ. Microbiol. 61: 526-530.

25. Jannasch, H. 1967. Growth of marine bacteria at limiting concentrations of organic carbon in seawater. Limnol. Oceanogr. 12: 264-271.

26. Kaiser, J-L, and K. W. Hanselmann. 1982. Fermentative metabolism of substituted monoaromatic compounds by a bacterial community from anaerobic sediments. Arch. Microbiol. 133: 384-391.

27. Kasper, H. F., and K. Wuhrmann. 1978. Product inhibition in sludge digestion. Microb. Ecol. 4: 241-248.

28. Lovley, D. R. 1985. Minimum threshold for metabolism in methanogenic bacteria. Appl. Environ. Microbiol. 149:1530-1531.

29. Lowry, O. H., N. J. Rosebrough, A. L. Farr, and R. J. Randall. 1951. Protein measurement with Folin phenol reagent. J. Biol. Chem. 193: 265-275.

30. McInerney, M. J., and M. P. Bryant. 1981. Basic principles of bioconversion in anaerobic digestion and methanogenesis. pp. 277-296. In S. S. Sofer, and O. R. Zoborsky (eds.), Biomass conversions for energy and fuels. Plenum publishing Corp.., New York.

31. McInerney, M. J., M. P. Bryant, R. B. Hespell, and J. W. Costerton. 1981. *Syntrophomonas wolfei* gen. nov., sp. nov., an anaerobic, syntrophic, fatty acid-oxidizing bacterium. Appl. Environ. Microbiol. 41: 1029-1039.

32. McInerney, M. J., M. P. Bryant, and N. Pfennig. 1979. An anaerobic bacterium that degrades fatty acids in syntrophic association with methanogens. Arch. Microbiol. 122: 129-135.

33. Min, H. and S. H. Zinder. 1989. Kinetics of acetate utilization by two thermophilic acetotrophic methanogens: *Methanosarcina* sp. strain CALS-1 and *Methanothrix* sp. strain CALS-1. Appl. Environ. Microbiol. 55: 488-491.

34. Mountfort, D. O., and M. P. Bryant. 1982. Isolation and characterization of an anaerobic syntrophic benzoate-degrading bacterium from sewage sludge. Arch. Microbiol. 133: 249-256.

35. Naggle, J. H. 1989. Physical Chemistry. IInd Ed. Scott, Foresman and Company, USA

36. Poels, J., P. van Assche, and W. Verstraete. 1985. Influence of H_2 stripping on methane production in conventional digestors. Biotech. Bioengr. 27: 1692-1698.

37. Powell, G. E. 1984. Equalisation of specific growth rates for syntrophic associations in batch cultures. J. Chem. Technol. Biotechnol. 34B: 97-100.

38. Powell, G. E. 1985. Stable coexistence of syntrophic associations in continuous culture. J. Chem. Technol. Biotechnol. 35B: 46-50.

39. Roberts, D. V. 1977. Enzyme kinetics. Cambridge University Press, Cambridge.

40. Robinson, J. A., and J. M. Tiedje. 1984. Competition between sulfate-reducing and methanogenic bacteria for H_2 under resting and growing conditions. Arch. Microbiol. 137: 26-32.

41. Seiler, W., H. Giehl, and P. Roggendorf. 1980. Detection of carbon monoxide and hydrogen by conversion of mercury oxide to mercury vapor. Atmos. Technol. 12: 40-45.

42. Schink, B. 1991. Syntrophism among prokaryotes, pp. 276-299. In: A. Balows, H. G. Truper, M. Dworkin, W. Harder, and K.-H. Schleifer (eds.), The prokaryotes, 2nd Ed. A handbook on the biology of bacteria: ecophysiology, isolation, identification, and applications. Springer-Verlag, New York.

43. Seitz, H.-J., B. Shink, and R. Conrad. 1990a. Energetics of syntrophic ethanol oxidation in defined chemostat cocultures. 1. Energy requirement for H_2 production and H_2 oxidation. Arch. Microbiol. 155: 82-88.

44. Seitz, H.- J., B. Schink, N. Pfennig, and R. Conrad. 1990b. Energetics of syntrophic ethanol oxidation in defined chemostat cocultures. 2. Energy sharing in biomass production. Arch. Microbiol. 155: 82-88.

45. Shelton, D. R., and J. M. Tiedje. 1984. Isolation and partial characterization of bacteria in an anaerobic consortium that mineralizes 3-chlorobenzoic acid. Appl. Environ. Microbiol. 48: 840-848.

46. Sleat, R., and J. P. Robinson. 1983. Methanogenic degradation of sodium benzoate in produndal sediments from a small eutrophic lake. J. Gen. Microbiol. 129: 141-152.

47. Smith, D. P., and P. L. McCarty. 1989. Energetics and the rate effects in the methanogenesis of ethanol and propionate in perturbed CSTR's. Biotech. Bioeng. 34: 39-47.

48. Suflita, J, . M., W. J. Smolenski, and J. A. Robinson. 1987. Alternative nonlinear model for estimating second-order rate coefficient for biodegradation. Appl. Environ. Microbiol. 53: 1064-1068.

49. Szewzyk, U., and B. Schink. 1989. Degradation of hydroquinone, gentisate, and benzoate by a fermenting bacterium in pure and defined mixed culture. Arch. Microbiol. 151: 541-545.

50. Thauer, R. K., and J. G. Morris. 1984. Metabolism of chemotrophic anaerobes: old views and new aspects. Symp. Soc. Gen. Microbiol. 36: 123-168.

51. Theile, J., W.-W. Wu, M. K. Jain, and J. G. Zeikus. 1990. Ecoengineering high rate anaerobic digestion systems: analysis of improved syntrophic biomethanation catalysts. Biotech. Bioeng. 35: 990-999.

52. Theile, J. H., and J. G. Zeikus. 1988. Control of interspecies flow during anaerobic digestion: significance of formate versus hydrogen transfer during syntrophic methanogenesis in flocs. Appl. Environ. Microbiol. 54: 20-29.

53. Westermann, P., B. K. Ahring, and R. A. Mah. 1989. Threshold acetate concentrations for acetate catabolism by acetoclastic methanogenic bacteria. Appl. Environ. Microbiol. 55: 514-515.

54. Young, L. Y. 1984. Anaerobic degrdation of aromatic compounds, p. 487-583. *In* D. T. Gibson (ed.), Microbial degradation of organic compounds. Marcel Dekker, New York.

Table 1. The effect of acetate on the benzoate threshold value and the energetics of benzoate degradation by cell suspensions of strain SB with *Desulfovibrio* strain G-11[a].

Additions	Final concentrations				$\Delta G'$ [b]
	Benzoate	Acetate	Hydrogen	Formate	
(mM)	(μM)	(mM)	(Pa)	(μM)	(kJ mol^{-1})
Acetate					
0.0	<0.2	3.0 (0.6)	0.21 (0.06)	8.95 (0.0)	-42.2 (2.8)
10.0	<0.2	13.2 (1.5)	0.08 (0.09)	7.13 (1.6)	-36.4 (1.9)
20.0	2.3 (0.5)	22.0 (2.5)	0.40 (0.03)	8.07 (0.5)	-30.1 (2.0)
65.0	29.8 (0.5)	65.7 (0.2)	0.30 (0.10)	7.22 (1.5)	-30.5 (0.8)
Sodium chloride					
65.0	<0.2	3.1 (0.0)	0.22 (0.0)	9.1 (0.4)	-41.5 (0)

[a] Values are means with the ranges given in parentheses.

[b] A value of 0.1 μM of benzoate was assumed in the calculations where final benzoate concentration was below detection limit.

Table 2. The effect of acetate removal on the benzoate threshold value for the coculture of strain SB and *Desulfovibrio* strain G-11.

D. baarsii present[a]	Benzoate concentration[b]		Final acetate concentration[b]	Final hydrogen concentration[b]
	Before (μM)	After (μM)	(mM)	(Pa)
No	3.7 (0.2)	3.7 (0.2)	20.3 (2.7)	0.32 (0.0)
Yes	7.1 (2.0)	<0.2	9.8 (0.4)	0.20 (0.1)

[a] Cell suspensions contained strain SB and *Desulfovibrio* strain G-11 and were amended with 20.0 mM acetate and 200 μM benzoate. After benzoate was degraded to a threshold concentration, a washed cell supension of *Desulfoarculus baarsii* was added to two of the four SB/G-11 cell suspensions.

[b] Values are means with the ranges given in parentheses.

Table 3. The effect of acetate concentration on the kinetic parameters for benzoate degradation by the coculture of strain SB and *Desulfovibrio* strain G-11.

Additions (mM)	apparent V_{max}[a] (nmol min^{-1} mg^{-1})	apparent K_m[a] (μM)	V_{max}/K_m[b] (min^{-1})
Acetate			
0.0	110.9 (5.3)	41.7 (3.9)	2.6
10.0	50.9 (2.8)	20.5 (2.8)	2.3
20.0	37.7 (2.1)	14.2 (2.1)	2.4
65.0	15.9 (1.3)	7.2 (0.9)	2.4
Sodium chloride			
65.0	99.8 (0.0)	44.6 (0.0)	2.2

[a] Values are means with the ranges given in parentheses.

[b] Corrected for 1 mg min^{-1} of protein.

Table 4. The effect of different terminal electron acceptors on the benzoate threshold value and the kinetic parameters for benzoate degradation by the coculture of strain SB and *Desulfovibrio* strain G-11.

Acetate added (mM)	Electron acceptor	Apparent kinetic values [a]		V_{max}/K_m [b]	Final benzoate concentration [a]
		V_{max} (nmol min^{-1} mg^{-1})	K_m (μM)	(min^{-1})	(μM)
20.0	sulfate	37.7 (2.1)	14.2 (2.1)	2.4	2.3 (0.5)
20.0	nitrate	20.7 (0.0)	18.2 (0.0)	1.1	<0.2

[a] Values are means with the ranges given in parentheses. Data for the condition when sulfate was the terminal electron acceptor are from Table 3.

[b] Corrected to 1 mg min^{-1} of protein.

Table 5. Effect of different *Desufovibrio* strains on the kinetics and energetics of benzoate degradation by strain SB.

Strain [a]	Acetate (mM)	Apparent values for benzoate degradation [b]			$\Delta G'$ [b] (kJ mol^{-1})
		V_{max} (nmol min^{-1} mg^{-1})	K_m (µM)	V_{max}/K_m [c] (min^{-1})	
G-11	0	110.9 (5.3)	41.7 (3.9)	2.6	-42.1 (2.8)
	10	50.9 (2.8)	20.5 (2.8)	2.5	-36.4 (1.9)
DG2	0	3.0 (0.1)	8.7 (1.8)	0.3	-39.9 (2.1)
	10	0.7 (0.3)	1.3 (0.2)	0.5	-38.9 (2.2)

[a] Data for strain G-11 are from Table 3.

[b] Values are means with the ranges given in parentheses.

[c] Corrected for 1 mg min^{-1} of protein.

Figure 1. Progress curves of benzoate degradation by washed cell suspensions of SB/G-11 cocultures without acetate added (o) and with 65 mM acetate (•). The protein concentrations in cell suspensions with and without acetate were 58.7 and 50.9 $\mu g\ ml^{-1}$, respectively.

Figure 2. Simulation of acetate inhibition of benzoate degradation by the competitive (Δ), noncompetitive (Δ), uncompetitive (o), and mixed (□) inhibition models with 65 mM acetate. The experimental data (•) obtained with 65 mM acetate is shown for comparison. The simulated curves were generated using the equations given below and the kinetic parameters determined from experiments without acetate amendment. Equation 4 was modified to include inhibition terms as follows: competitive, $V_{max}\ t = S_o - S + [(K_m + S_c)\ (1+I/K_i)]\ \ln\ [(S_c - S_o)/(S_c - S)]$; noncompetitive, $[V_{max}/(1+I/K_i)]\ t = S_o - S + (K_m + S_c)\ \ln\ [(S_c - S_o)/(S_c - S)]$; uncompetitive, $[V_{max}/(1+I/K_i)]\ t = S_o - S + [(K_m + S_c)/(1+I/K_i)]\ \ln\ [(S_c - S_o)/(S_c - S)]$; and mixed, $[V_{max}/(1+I/K_i)]\ t = S_o - S + [(K_m + S_c)\ (1+I/K_i)]\ \ln\ [(S_c - S_o)/(S_c - S)]$.

Figure 3. Simulation study to determine whether acetate inhibition results in a threshold for benzoate degradation. The simulated benzoate degradation curve (•) was generated using equation 4 modified to include a term for uncompetitive inhibition (see legend to Fig. 2) and the values for V_{max}, K_m, K_i, and S_o obtained from experiments with 65 mM acetate. The experimental progress curve (o) obtained with 65 mM acetate is shown for comparison.

Figure 4. Comparison between experimental (•) and predicted (o) benzoate threshold values for the coculture of strain SB and *Desulfovibrio* strain G-11 at different initial acetate concentrations. The predicted benzoate threshold values

were calculated using equation 7 and experimentally determined final acetate, formate, and H_2 concentrations.

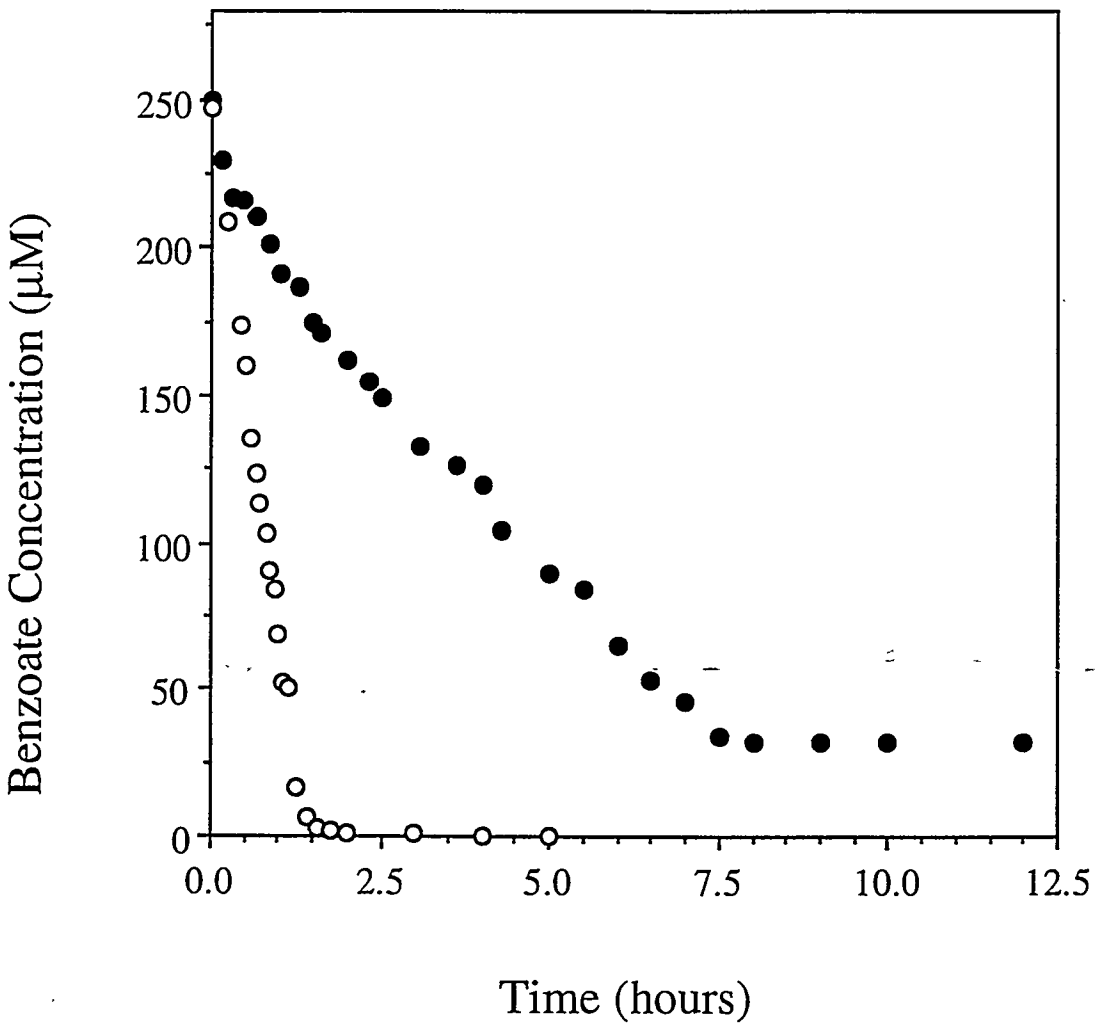
Benzoate Concentration (μM)
250
200
150
100
50
0
0.0
2.5
5.0
7.5
10.0
12.5
Time (hours)

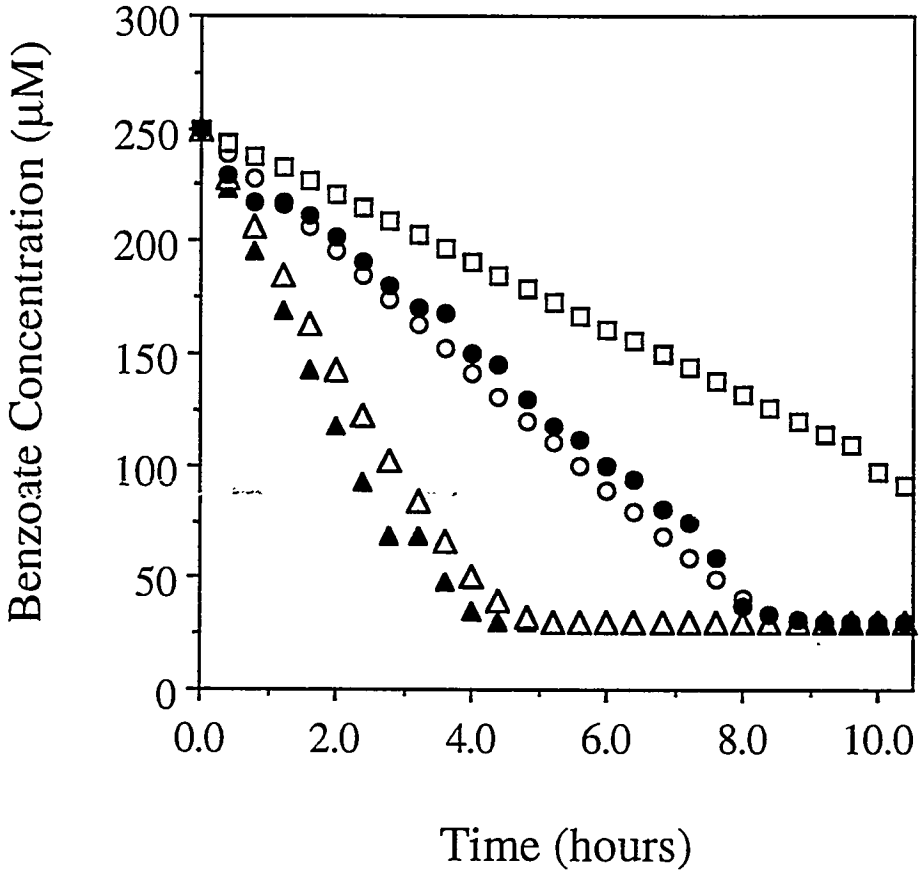
Benzoate Concentration (μM)
300
250
200
150
100
50
0
0.0
2.0
4.0
6.0
8.0
10.0
Time (hours)

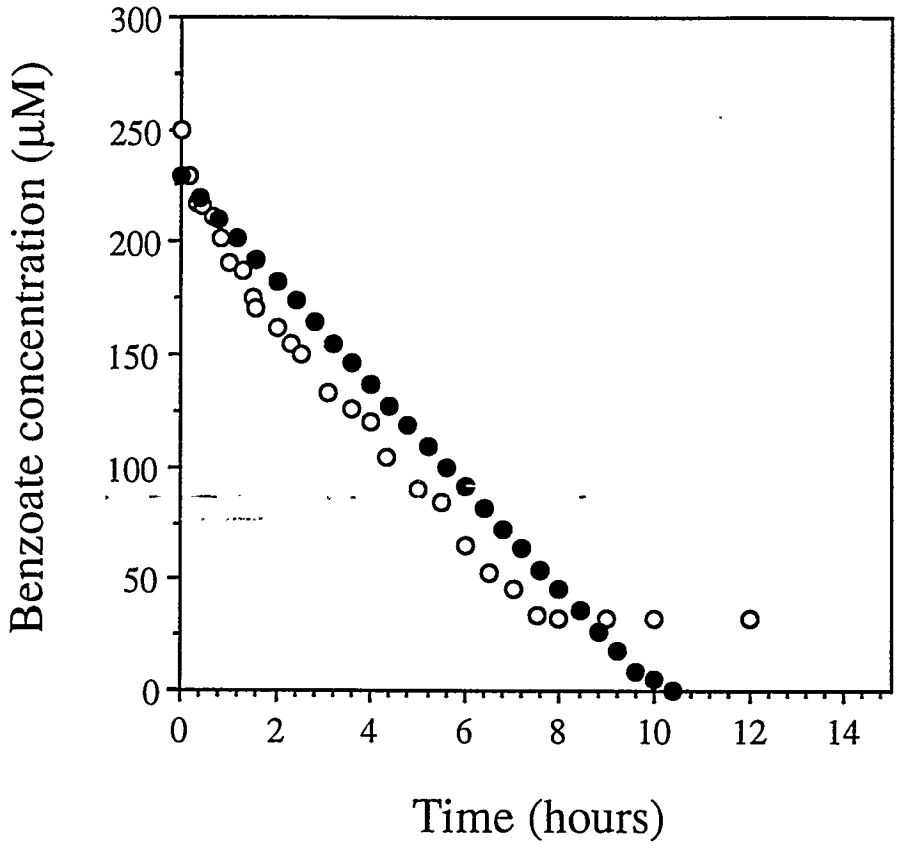
Benzoate concentration (µM)
300
250
200
150
100
50
0
0
2
4
6
8
10
12
14
Time (hours)